Inorg. Chem. **2008**, *47*, 8736−8747

Copper−Hydroperoxo-Mediated N-Debenzylation Chemistry Mimicking Aspects of Copper Monooxygenases

Debabrata Maiti, Amy A. Narducci Sarjeant, and Kenneth D. Karlin*

Department of Chemistry, The Johns Hopkins University, Baltimore, Maryland 21218

Received April 5, 2008

A substantial oxidative N-debenzylation reaction along with PhCH═O formation occurs from a hydroperoxo−copper(II) complex that has a dibenzylamino substrate (—$N(CH_2Ph)_2$ appended as a substituent on one pyridyl group of its tripodal tetradentate TMPA (also TPA, (2-pyridylmethyl)amine)) ligand framework. During the course of the ($L^{N(CH_2Ph)_2}$)$Cu^{II}(^{-}OOH)$ reactivity, the formation of a substrate and a $^{-}$OOH-derived (an oxygen atom) alkoxo $Cu^{II}(^{-}OR)$ complex occurs. The observation that the same $Cu^{II}(^{-}OR)$ species occurs from Cu^{I}/PhIO chemistry suggests the possibility that a copper−oxo (cupryl) reactive intermediate forms during the alkoxo species formation; new ESI-MS data provide further support for this high-valent intermediate. A net H atom abstraction chemistry is proposed on the basis of the kinetic isotope effect studies provided here and the previously published study for a closely related $Cu^{II}(^{-}OOH)$ species incorporating dimethylamine (—$N(CH_3)_2$) as the internal substrate;[27] the Cu^{I}/PhIO reactivity with similar isotope effect results provides further support. The reactivity of these chemical systems closely resembles the proposed oxidative N-dealkylation mechanisms that are effected by the copper monooxygenases, dopamine β-monooxygenase (DβM) and peptidylglycine-α-hydroxylating monooxygenase (PHM).

Introduction

The study of copper(I)-dioxygen adducts and their (reduced) derivatives is of considerable current interest.[1−8] In large part, these efforts comprise the desire to elucidate fundamental aspects such as the structural type along with associated spectroscopy, electronic structure, and, of course, reactivity patterns. Inspirations for such investigations also come from aspects of bioinorganic chemistry; we wish to provide fundamental information that may be relevant to copper metalloenzyme active sites, where the processing of molecular oxygen occurs. Included in the latter are the copper monooxygenases, peptidylglycine-α-hydroxylating monooxygenase (PHM) and dopamine β-monooxygenase (DβM), which are mammalian proteins that serve in the biosynthesis of various neuropeptides or hormones.[9−12] Figure 1 outlines the specific reactions that are carried out. Each involves an

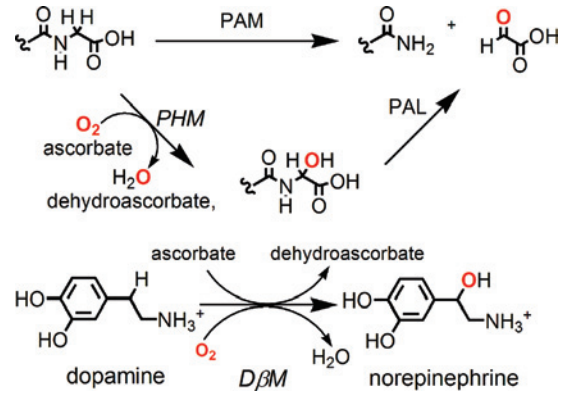

Figure 1. Homologus copper protein DβM (bottom), which transforms dopamine to norepinephrine, and homologous copper protein PHM (top), which hydroxylates the C-terminus of the peptide backbone, a process that is followed by N-dealkylation by PAL.

* To whom correspondence should be addressed. E-mail: karlin@jhu.edu.

(1) Itoh, S.; Fukuzumi, S. *Acc. Chem. Res.* **2007**, *40*, 592–600.
(2) Cramer, C.; Tolman, W. *Acc. Chem. Res.* **2007**, *40*, 601–608.
(3) Suzuki, M. *Acc. Chem. Res.* **2007**, *40*, 609–617.
(4) Itoh, S. *Curr. Opin. Chem. Biol.* **2006**, *10*, 115–122.
(5) Quant Hatcher, L.; Karlin, K. D. *J. Biol. Inorg. Chem.* **2004**, *9*, 669–683.
(6) Mirica, L. M.; Ottenwaelder, X.; Stack, T. D. P. *Chem. Rev.* **2004**, *104*, 1013–1045.
(7) Lewis, E. A.; Tolman, W. B. *Chem. Rev.* **2004**, *104*, 1047–1076.
(8) Rolff, M.; Tuczek, F. *Angew. Chem., Int. Ed.* **2008**, *47*, 2344–2347.
(9) Klinman, J. P. *J. Biol. Chem.* **2006**, *281*, 3013–3016.
(10) Bauman, A. T.; Yukl, E. T.; Alkevich, K.; McCormack, A. L.; Blackburn, N. J. *J. Biol. Chem.* **2006**, *281*, 4190–4198.
(11) Chen, P.; Solomon, E. I. *Proc. Natl. Acad. Sci. U.S.A.* **2004**, *101*, 13105–13110.
(12) Prigge, S. T.; Eipper, B.; Mains, R.; Amzel, L. M. *Science* **2004**, *304*, 864–867.

10.1021/ic800617m CCC: $40.75
Published on Web 09/11/2008

insertion of one oxygen atom (from O_2) into the substrate. For DβM, net benzylic hydroxylation occurs, whereas for PHM, hydroxylation is followed by N-dealkylation. The active sites of each enzyme are known to be very similar, and each contains two copper ions. Previous biophysical studies have shown these to be relatively far apart, and more recent X-ray crystallographic structures of PHM show them to be ∼11 Å apart.[12] Thus, the mechanism of action focuses on the copper chemistry taking place at one of the two copper ions Cu_M (≡ Cu_B), whereas the other copper ion Cu_H (≡ Cu_A) serves to transfer electrons.

Because of the history of biochemical/biophysical studies on these enzymes and in the context of considering various copper−dioxygen-derived species that are either known or unknown in inorganic chemistry, a hydroperoxo−copper(II) ($Cu^{II}(^{-}OOH)$) complex and a superoxo−copper(II) ($Cu^{II}(O_2^{\bullet -})$) complex derived from the initial $Cu^{I}-O_2$ chemistry or the high-valent cupryl [$Cu^{II}-O\bullet$] have been discussed as species that might be responsible for an initial hydrogen atom abstraction reaction.[2,4,8,9,11−18] For some time, a hydroperoxo complex was suggested, but more recently, both experimental and computational (bio)chemistry suggest that the $Cu^{II}(O_2^{\bullet -})$ moiety is relevant.[4,9−11,13] Furthermore, one crystal structure of PHM reveals what is best described as a $Cu_M^{II}(O_2^{\bullet -})$ moiety that is perfectly juxtaposed to the relevant substrate C−H bond. Other theoretical treatments prefer a prior (rather than subsequent) O−O cleavage from $Cu^{II}(^{-}OOH)$, which leads to a high-valent $[Cu-O]^{2+}$ or $[Cu-O]^{+}$ (equivalent to $Cu^{III}-O\bullet$) moiety (cupryl) that affects H atom transfer.[14,15] To obtain answers or to provide insight, synthetic bioinorganic chemists have been actively pursuing the chemistry of mononuclear copper−dioxygen-derived complexes, especially in the reactivity toward substrates.[2,19−27] Scheme 1 presents the several species that may affect H atom abstractions, which are followed

Scheme 1

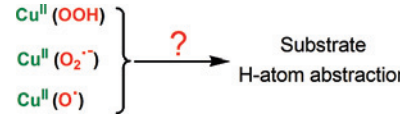

by the net transfer of an oxygen atom to the substrate (i.e., monooxygenase activity).

In biomimetic studies that are approached via coodination chemistry efforts, two types of hydroperoxide−copper species have been produced to date: μ-1,1-hydroperoxo-dicopper(II) complexes and mononuclear complexes. We have recently demonstrated substrate C−H activation chemistry starting from well-characterized dinuclear μ-($^{-}$OOH)-dicopper(II) complexes, oxidative N-dealkylation, or $RCH_2C{\equiv}N$ oxidative cleavage (to the RCH═O aldehyde and cyanide).[28,29] Suzuki has also observed a hydrocarbon attack from a $Cu^{II}_2(^{-}OH)_2$ and H_2O_2 reaction, which gives a $Cu^{II}-OOR_{ligand-substrate}$ product.[30] A number of well-characterized mononuclear $Cu^{II}(^{-}OOH)$ complexes have been described;[31−37] however, substrate oxidations have been limited to organic sulfides[37] or olefins (but in low yields).[32] In our own laboratories, we have in the last year been able to demonstrate C−H activation and thus oxygenation from $Cu^{II}(^{-}OOH)$ complexes, as further discussed. There have been notable advances in the generation of a mononuclear $Cu^{II}(O_2^{\bullet -})$ or $Cu^{III}(O_2^{2-})$ species,[2,24,25,38] but a chemistry in which such entities attack substrate C−H bonds has yet to be described. There are no discrete examples or direct evidence of mononuclear high-valent copper−oxo species; however, see the further discussion below.

Within the context of the introduction given above, we describe the chemistry of the new ligand $L^{N(CH_2Ph)_2}$ (Chart 1, below) and its copper-complex-promoted oxidative chemistry. Whereas the main focus is on a mononuclear $Cu^{II}(^{-}OOH)$ species, $[(L^{N(CH_2Ph)_2})Cu^{II}(^{-}OOH)]^{+}$ (**2**), we complement it with (ligand)$Cu^{I}-O_2$ reactivity and a separate attempt to interrogate the possible involvement of cupryl chemistry.

(13) Chen, P.; Solomon, E. I. *J. Am. Chem. Soc.* **2004**, *126*, 4991–5000.
(14) Yoshizawa, K.; Kihara, N.; Kamachi, T.; Shiota, Y. *Inorg. Chem.* **2006**, *45*, 3034–3041.
(15) Crespo, A.; Marti, M. A.; Roitberg, A. E.; Amzel, L. M.; Estrin, D. A. *J. Am. Chem. Soc.* **2006**, *128*, 12817–12828.
(16) Evans, J. P.; Ahn, K.; Klinman, J. P. *J. Biol. Chem.* **2003**, *278*, 49691–49698.
(17) Decker, A.; Solomon, E. I. *Curr. Opin. Chem. Biol.* **2005**, *9*, 152–163.
(18) Schröder, D.; Holthausen, M. C.; Schwarz, H. *J. Phys. Chem. B* **2004**, *108*, 14407–14416.
(19) Fujii, T.; Yamaguchi, S.; Hirota, S.; Masuda, H. *Dalton Trans.* **2008**, 164–170.
(20) Kunishita, A.; Ishimaru, H.; Nakashima, S.; Ogura, T.; Itoh, S. *J. Am. Chem. Soc.* **2008**, *130*, 4244–4245.
(21) Kunishita, A.; Teraoka, J.; Scanlon, J. D.; Matsumoto, T.; Suzuki, M.; Cramer, C. J.; Itoh, S. *J. Am. Chem. Soc.* **2007**, *129*, 7248–7249.
(22) Hong, S.; Huber, S. M.; Gagliardi, L.; Cramer, C. C.; Tolman, W. B. *J. Am. Chem. Soc.* **2007**, *129*, 14190–14192.
(23) Fujii, T.; Yamaguchi, S.; Funahashi, Y.; Ozawa, T.; Tosha, T.; Kitagawa, T.; Masuda, H. *Chem. Commun.* **2006**, 4428–4430.
(24) Maiti, D.; Lee, D.-H.; Gaoutchenova, K.; Würtele, C.; Holthausen, M. C.; Sarjeant, A. A. N.; Sundermeyer, J.; Schindler, S.; Karlin, K. D. *Angew. Chem., Int. Ed.* **2008**, *47*, 82–85.
(25) Maiti, D.; Fry, H. C.; Woertink, J. S.; Vance, M. A.; Solomon, E. I.; Karlin, K. D. *J. Am. Chem. Soc.* **2007**, *129*, 264–265.
(26) Maiti, D.; Lucas, H. R.; Narducci Sarjeant, A. A.; Karlin, K. D. *J. Am. Chem. Soc.* **2007**, *129*, 6998–6999.
(27) Maiti, D.; Narducci Sarjeant, A. A.; Karlin, K. D. *J. Am. Chem. Soc.* **2007**, *129*, 6720–6721.
(28) Li, L.; Narducci Sarjeant, A. A.; Karlin, K. D. *Inorg. Chem.* **2006**, *45*, 7160–7172.
(29) Li, L.; Narducci Sarjeant, A. A.; Vance, M. A.; Zakharov, L. N.; Rheingold, A. L.; Solomon, E. I.; Karlin, K. D. *J. Am. Chem. Soc.* **2005**, *127*, 15360–15361.
(30) Itoh, K.; Hayashi, H.; Furutachi, H.; Matsumoto, T.; Nagatomo, S.; Tosha, T.; Terada, S.; Fujinami, S.; Suzuki, M.; Kitagawa, T. *J. Am. Chem. Soc.* **2005**, *127*, 5212–5223.
(31) Kodera, M.; Kita, T.; Miura, I.; Nakayama, N.; Kawata, T.; Kano, K.; Hirota, S. *J. Am. Chem. Soc.* **2001**, *123*, 7715–7716.
(32) Ohta, T.; Tachiyama, T.; Yoshizawa, K.; Yamabe, T.; Uchida, T.; Kitagawa, T. *Inorg. Chem.* **2000**, *39*, 4358–4369.
(33) Wada, A.; Harata, M.; Hasegawa, K.; Jitsukawa, K.; Masuda, H.; Mukai, M.; Kitagawa, T.; Einaga, H. *Angew. Chem., Int. Ed.* **1998**, *37*, 798–799.
(34) Yamaguchi, S.; Wada, A.; Nagatomo, S.; Kitagawa, T.; Jitsukawa, K.; Masuda, H. *Chem. Lett.* **2004**, *33*, 1556–1557.
(35) Yamaguchi, S.; Nagatomo, S.; Kitagawa, T.; Funahashi, Y.; Ozawa, T.; Jitsukawa, K.; Masuda, H. *Inorg. Chem.* **2003**, *42*, 6968–6970.
(36) Yamaguchi, S.; Masuda, H. *Sci. Technol. Adv. Mater.* **2005**, *6*, 34–47.
(37) Fujii, T.; Naito, A.; Yamaguchi, S.; Wada, A.; Funahashi, Y.; Jitsukawa, K.; Nagatomo, S.; Kitagawa, T.; Masuda, H. *Chem. Commun.* **2003**, 2700–2701.
(38) Würtele, C.; Gaoutchenova, E.; Harms, K.; Holthausen, M. C.; Sundermeyer, J.; Schindler, S. *Angew. Chem., Int. Ed.* **2006**, *45*, 3867–3869.

This work follows our recent work in which we employed a close analog $[(L^{N(CH_3)_2})Cu^{II}(^{-}OOH)]^{+}$ (**3**), where both ligands are the derivatives of TMPA (also TPA, tris(2-pyridylmethyl)amine)) (Chart 1, below); this shows that the hydroperoxo group that is coordinated to copper(II) can affect oxidative N-dealkylation chemistry on the juxtaposed dimethylamino substrate.[27] In this Article, the chemistry of the $L^{N(CH_2Ph)_2}$ analog is fully described.

Experimental Section

Materials and Methods. Unless otherwise stated, all solvents and chemicals used were commercially available analytical grade. Acetone, diethyl ether, pentane, propionitrile, methanol, and tetrahydrofuran (THF) were used after being passed through a 60-cm-long column of activated alumina (Innovative Technologies) under argon. The deoxygenation of solvents was affected either by repeated freeze/pump/thaw cycles or by bubbling with argon for 30−45 min. Dioxygen was dried by being passed through a short column of supported P_4O_{10} (Aquasorb, Mallinckrodt). The preparation and handling of air-sensitive compounds were performed under an argon atmosphere and by the use of standard Schlenk techniques or in an MBraun Labmaster 130 inert-atmosphere (<1 ppm O_2, <1 ppm H_2O) drybox filled with nitrogen. Elemental analyses were performed by Desert Analytics (Tucson, AZ). ^{1}H NMR and ^{13}C NMR spectra were measured on a Bruker 400 MHz spectrometer. Chemical shifts were reported as δ values relative to an internal standard (Me_4Si) and the residual-solvent proton peak. Ultraviolet−visible spectra were recorded on a Hewlett-Packard model 8453A diode-array spectrophotometer equipped with a two-window quartz H. S. Martin Dewar filled with cold MeOH (25 to −85 °C) maintained and controlled by a Neslab ULT-95 low-temperature circulator. The spectrophotometer cells that were used were made by Quark Glass, and each had a column, a pressure/vacuum side stopcock, and a path length of 2 mm. The copper complexes are ClO_4^- and $B(C_6F_5)_4^-$ salt complexes unless otherwise stated. **Caution!** *Whereas we have experienced no problems in working with perchlorate compounds, they are potentially explosive, and care must be taken to refrain from working with large quantities*. Electrospray ionization mass spectra were acquired by the use of a Finnigan LCQ Deca ion-trap mass spectrometer equipped with an electrospray ionization source (Thermo Finnigan, San Jose, CA). For metastable species (as described below), samples were introduced from low-temperature solutions with a liquid-N_2 precooled plastic syringe and were quickly injected into the instrument sample port that feeds the instrument syringe pump, which operates at 10 μL/min via a silica capillary line. The heated capillary temperature was 250 °C, and the spray voltage was 5 kV. X-ray diffraction was performed at the X-ray diffraction facility at The Johns Hopkins University. The X-ray intensity data were measured on an Oxford Diffraction Xcalibur 3 system equipped with a graphite monochromator, an Enhance (Mo) X-ray source (λ = 0.71073Å) that was operated at 2 kW (50 kV, 40 mA), and a CCD detector. The frames were integrated with the Oxford Diffraction CrysAlisRED software package. X-band electron paramagnetic resonance (EPR) spectra were recorded on a Bruker EMX CW EPR spectrometer that was controlled with a Bruker ER 041 XG microwave bridge operating at the X band (~9 GHz). The low-temperature experiments were carried out via a N_2(l) finger Dewar.

Synthesis of $[(L^{N(CH_2Ph)_2})Cu^{II}(H_2O)(ClO_4)]^{+}$ (1). The synthesis and characterization of $L^{N(CH_2Ph)_2}$ was recently reported.[39] Ligand $L^{N(CH_2Ph)_2}$ (0.250 g, 0.515 mmol) was treated with $Cu^{II}(ClO_4)_2\cdot 6H_2O$ (0.191 g, 0.516 mmol) (Aldrich) in acetone (10 mL) and was stirred for 25 min at room temperature. The complex was precipitated as a greenish-blue solid upon the addition of Et_2O (140 mL). The supernatant was decanted, and the resulting crystalline solid was washed two times with Et_2O and was dried under vacuum to afford $[(L^{N(CH_2Ph)_2})Cu^{II}(H_2O)(ClO_4)]ClO_4$(acetone) (**1**) (0.305 g, 72% yield). Single crystals were obtained by the vapor diffusion of Et_2O into a solution of the complex in acetone. Anal. Calcd for $[(L^{N(CH_2Ph)_2})Cu^{II}(H_2O)(ClO_4)]ClO_4$(acetone), $C_{35}H_{39}Cl_2CuN_5O_{10}$: C, 51.01; H, 4.77; N, 8.50. Found: C, 50.88; H, 4.88; N, 8.37. X-band EPR in acetone at 77 K: $g_{||} = 2.252$, $g_{\perp} = 2.047$, $A_{||} = 170$ G, $A_{\perp} = 29.5$ G.

Generation of $[(L^{N(CH_2Ph)_2})Cu^{II}(^{-}OOH)]^{+}$ (2) and Reactivity Study. In 20 mL of acetone solution, complex **1** (0.337 g, 0.409 mmol) was dissolved and was cooled to −80 °C by the use of an acetone/dry ice bath. The addition of Et_3N (0.412 g, 4.08 mmol) and 50 wt % H_2O_2 (252 μL, 4.09 mmol) (Aldrich) led to the formation of the green complex $[(L^{N(CH_2Ph)_2})Cu^{II}(^{-}OOH)]ClO_4$ (**2**) (λ = 380 nm, ε = 1400 $M^{-1}cm^{-1}$). When an aliquot of this −80 °C green solution was injected into the mass spectrometer, a parent peak cluster at m/z = 581.03 that corresponded to the positive ion $[(L^{N(CH_2Ph)_2})Cu^{II}(OOH)]^{+}$ was observed. When $H_2{}^{18}O_2$ was used for the formation of complex **2**, the positive ion peak clusters shifted to m/z = 585.09. The alkoxide product $[(L^{N(CH_2Ph)_2})Cu^{II}(OOH)]^{+}$ (**2**) was detected with a parent peak cluster at m/z = 563.05 that corresponded to the positive ion $[(L^{N(CH_2Ph)(PhCHO^{-})})Cu^{II}]^{+}$ (**4**). An EPR spectrum of the reaction mixture containing complex **4** reveals typical Cu(II) axial species supporting its mononuclear formulation. When the formation of complex **2** was carried out with $H_2{}^{18}O_2$, the positive ion peak clusters of complex **4** shifted to m/z = 565.20. X-band EPR of complex **2** in acetone at 77 K: $g_{||} = 2.240$, $g_{\perp} = 2.041$, $A_{||} = 180$ G, $A_{\perp} = 27$ G. The hydroperoxo species $[(L^{N(CH_2Ph)_2})Cu^{II}(^{-}OOH)]ClO_4$ (**2**) was kept at −80 °C and was stirred for 15 min. Upon warming, the solution was carefully concentrated to 4 mL under vacuum, and the ESI-MS of the reaction solution was recorded. The resulting copper solution was washed three times with Et_2O (200 mL) whereupon the Et_2O solutions were combined and dried over Na_2SO_4. The Et_2O solution was analyzed by GC and GC-MS (see below for conditions), which confirmed the formation of PhCHO (authentic commercial PhCHO was also used for the comparison) (43% yield). When the formation of complex **2** was carried out with $H_2{}^{18}O_2$ and similar follow-up procedures were performed, ~65% ^{18}O-atom incorporation in PhCHO occurred.

Isolation of Organic Products. After a washing with Et_2O, the residual material was treated with 250 mL of saturated Na_2EDTA/H_2O solution, and the organic part was extracted by using 80 mL of CH_2Cl_2. The $CH_2Cl_2/Na_2EDTA/H_2O$ extraction was repeated three times to ensure complete demetalation. The organic CH_2Cl_2 solution was dried over anhydrous Na_2SO_4, was filtered, and was concentrated by rotory evaporation. The ESI-MS of the organic extract was recorded. The isolation and purification by column chromatography (with Al_2O_3, 2% MeOH + CH_2Cl_2) revealed unreacted $L^{N(CH_2Ph)_2}$ (0.032 g, ~16%) and the N-debenzylated product $L^{NH(CH_2Ph)}$ (0.077 g, ~48%). The products were characterized by ESI-MS, ^{1}H NMR, ^{13}C NMR, and thin-layer chromatography (TLC). The formation of $L^{N(CH_2Ph)(COPh)}$ and $L^{N(COPh)_2}$ (0.014 g, ~7%; ESI-MS: 522.53 (M + Na) and 536.31 (M + Na), respectively) and $L^{NH(COPh)}$ (0.004 g, ~3%; ESI-MS: 410.65 (M + H) and 432.51 (M + Na)) was also observed. Several attempts to isolate these organic products in an absolute pure form were unsuccessful because of their comparable R_f values; however, their formulation can be confirmed from both pre- and postdemetalation. We did not find any evidence of L^{NH_2} formation.

Experiment Adding Only One Equivalent Peroxide. Triethylamine (Et_3N, 0.041 g, 0.408 mmol) and 50 wt % H_2O_2 (25 μL, 0.408 mmol) were added to the 20 mL of acetone solution (−80 °C) of complex **1** (0.337 g, 0.409 mmol). Our following procedures similar to those described above produced unreacted $L^{N(CH_2Ph)_2}$(0.130 g, ∼65%), $L^{NH(CH_2Ph)}$ (0.026 g, ∼16%), and $L^{N(CH_2Ph)\text{-}(COPh)}$ plus $L^{N(COPh)_2}$ (0.002 g, ∼1%). A similar reaction in methanol as the solvent lead to the formation of ∼14% $L^{NH(CH_2Ph)}$, <1% $L^{N(CH_2Ph)(COPh)}$, and $L^{N(CH_2Ph)_2}$ in ∼68% yield. The starting ligand $L^{N(CH_2Ph)_2}$ was obtained in ∼64% yield along with ∼14% $L^{NH(CH_2Ph)}$ and <1% $L^{N(CH_2Ph)(COPh)}$ in propionitrile as the solvent for an analogous $[(L^{N(CH_2Ph)_2})Cu^{II}(H_2O)(ClO_4)]^+$ (**1**)/H_2O_2/Et_3N reaction.

$L^{NH(CH_2Ph)}$. ^{1}H NMR ($CDCl_3$, δ): 3.70 (s, 2H, CH_2Py), 3.89 (s, 4H, $2CH_2Py$), 4.48 (d, 2H, CH_2Ph), 5.13 (s, 1H, NH), 6.22 (d, 1H), 6.83 (d, 1H), 7.09 (t, 2H), 7.11−7.44 (m, 5H), 7.45−7.68 (m, 5H), 8.49 (d, 2H). ^{13}C NMR ($CDCl_3$, δ): 46.51, 60.21, 77.39, 104.74, 112.04, 121.86, 122.83, 126.79, 127.41, 128.55, 136.38, 137.89, 139.43, 143.28, 148.99, 157.76, 158.29, 159.84. ESI-MS: 396.68 (M + H), 418.33 (M + Na). R_f = 0.23, alumina, 2% MeOH + CH_2Cl_2.

Reaction of $[(L^{N(CH_2Ph)_2})Cu^{I}]^+$ (6) with O_2. The synthesis and characterization of the copper(I) complex $[(L^{N(CH_2Ph)_2})Cu^{I}]B(C_6F_5)_4$ (**6**) was previously reported.[39] The formation of the bis(μ-oxo)dicopper(III) complex $[((L^{N(CH_2Ph)_2})Cu^{III})_2(O^{2-})_2](B(C_6F_5)_4)_2$ (**9**) from the O_2 reactivity of complex **6** was confirmed by low-temperature UV−vis and resonance Raman (rR) spectroscopy. For the determination of ligand oxidation chemistry, a solution of $[(L^{N(CH_2Ph)_2})Cu^{I}]^+$ (**6**) (0.125 g, 0.101 mmol) in a 25 mL Schlenk flask with 6 mL of Et_2O was prepared in the glovebox. The removal to the benchtop and the cooling to −80 °C, followed by the bubbling of O_2 via a long syringe needle (20 s), was carried out, and this was followed by the removal of excess dioxygen via evacuation and purging with argon. After 30 min, the solution was warmed to room temperature, and demetalation procedures with Na_2EDTA/H_2O/CH_2Cl_2 were performed; this resulted in the production of dipicolylamine (0.001 g, ∼4%), $L^{NH(CH_2Ph)}$ (0.002 g, ∼5%), and unreacted $L^{N(CH_2Ph)_2}$ (0.037 g, ∼75%).

Synthesis of $[L^{NH(CH_2Ph)})Cu^{II}(Cl)]^+$ (10). We followed the synthetic procedures that were previously employed in generating crystalline copper(II)−chloride complexes via ligand−Cu(I)−$CHCl_3$ chemistry.[27,40] Isolated $L^{NH(CH_2Ph)}$ (0.050 g, 0.126 mmol) and $[Cu^{I}(CH_3CN)_4]ClO_4$ (0.042 g, 0.128 mmol) were placed in a 25 mL Schlenk flask under argon. Dioxygen-free CH_3CN (2 mL) was added under argon to form a yellow solution, and this was stirred for 10 min. Deoxygenated $CHCl_3$ (0.3 mL) was then added under argon whereupon the solution ceased to look transparent and turned green. After 2 h, 20 mL of Et_2O was added to precipitate the copper complex. X-ray-quality crystals of this compound, $[(L^{NH(CH_2Ph)})Cu^{II}(Cl)]^+$ (**10**), were obtained from the reaction solution after the precipitation that was prompted by Et_2O. The green precipitate was recrystallized two times from CH_3CN/Et_2O. Anal. Calcd for $C_{25}H_{29}Cl_2CuN_5O_6$: C, 47.66; H, 4.64; N, 11.12. Found: C, 47.71; H, 4.34; N, 11.08. After the vacuum drying, the green crystals weighed 0.054 g (68%).

Reaction of $[(L^{N(CH_2Ph)_2})Cu^{I}]B(C_6F_5)_4$ (6) with PhIO. $[(L^{N(CH_2Ph)_2})Cu^{I}]B(C_6F_5)_4$ (**6**)[39] (0.018 g, 0.015 mmol) was dissolved in 18 mL of CH_3CN inside the drybox and was taken in a 25 mL Schlenk flask. In a separate Schlenk flask, PhIO (0.033 g, 0.150 mmol) was taken with 4.0 mL of CH_3CN under argon and was stirred for 30 min and cooled to −40 °C. Via a syringe, 1 mL of this CH_3CN solution was introduced anaerobically into the −40 °C solution of complex **6**. The ESI-MS of this low-temperature copper solution was recorded and showed the initial strong peak at m/z = 564.25 because of high-valent $[(L^{N(CH_2Ph)_2})Cu^{III}{=}O]^+$species formation. The decomposition of this 564 species was followed with respect to time, which leads to the alkoxo species $[(L^{N(CH_2Ph)(PhCHO^-)})Cu^{II}]^+$ (**4**) (m/z = 563.18). When the formation of complex **4** was carried out with PhIO plus $H_2{}^{18}O$, the positive ion peak clusters of complex **4** shifted to m/z = 565.34.

Reaction of $[(L^{N(CH_3)_2})Cu^{I}]B(C_6F_5)_4$ (7)[39] with PhIO. $[(L^{N(CH_3)_2})Cu^{I}]B(C_6F_5)_4$ (**7**) (0.015 g, 0.014 mmol) was dissolved in 15 mL of CH_3CN inside the drybox and was taken in a 25 mL Schlenk flask. In a separate Schlenk flask, PhIO (0.031 g, 0.140 mmol) was taken with 5.0 mL of CH_3CN under argon and was stirred for 30 min. Via a syringe, 1 mL of this CH_3CN solution (−40 °C) was introduced anaerobically into the −40 °C solution of complex **7**. The ESI-MS of the low-temperature copper solution was recorded, and it showed the strong peak at m/z = 411.18. When a similar reaction was carried out with $[(L^{N(CH_3)(CD_3)})Cu^{I}]^+$and PhIO, the positive ion peak clusters contained dominant peaks at m/z = 413.24 and 414.14 because of the generation of $[(L^{N(CH_3)(CD_2O^-)})Cu^{I}]^+$ and $[(L^{N(CD_3)(CH_2O^-)})Cu^{I}]^+$, respectively.

Chemistry of $[(L^{N(CH_3)_2})Cu^{II}(^-OOH)]^+$ (3) and its Reactivity Study. The synthesis, characterization, and reactivity studies of the copper(II)−hydroperoxo complex $[(L^{N(CH_3)_2})Cu^{II}(^-OOH)]ClO_4$ (**3**) were previously reported.[27] Via a further examination in the present study, we were able to isolate a small amount of one decomposition product, $[(L^{N(CH_3)_2})Cu^{II}(HCOO^-)(ClO_4)Cu^{II}{-}(L^{NH(CH_3)})](ClO_4)_2$ (**11**), with dicopper(II) centers bridged by the ($HCOO^-$) group from the reactivity of complex **3** in acetone. Compound **11** was characterized crystallographically, and its EPR and ESI-MS characterization studies were performed. (See Supporting Information.) We also previously described the chemistry of $[(L^{N(CH_3)(CD_3)})Cu^{II}(^-OOH)]^+$ (**3-CD$_3$**)[27] for which we now find that the extracted unreacted ligand has its isotope label scrambled. (See the discussion below.)

Results and Discussion

Ligand Design and Hydroperoxo−Copper(II) Complexes. We have previously carried out and published extensive studies concerning the dioxygen reactivity of the parent-ligand copper(I) complex $[(TMPA)Cu^{I}(CH_3CN)]^+$ along with a variety of analogs.[41–43] Masuda and coworkers[44,45] elaborated on the TMPA framework by inputting potential hydrogen-bonding moieties and placing them in 6-pyridyl positions. In a series of studies, they showed that ligand−copper(I) compounds react with O_2 to form binuclear copper−dioxygen adducts (formally μ-1,2-peroxodicopper(II) complexes) that do show altered UV−vis and rR spectro-

(39) Maiti, D.; Woertink, J. S.; Narducci Sarjeant, A. A.; Solomon, E. I.; Karlin, K. D. *Inorg. Chem.* **2008**, *47*, 3787–3800.
(40) Lucchese, B.; Humphreys, K. J.; Lee, D.-H.; Incarvito, C. D.; Sommer, R. D.; Rheingold, A. L.; Karlin, K. D. *Inorg. Chem.* **2004**, *43*, 5987–5998.
(41) Hatcher, L. Q.; Karlin, K. D. *Adv. Inorg. Chem.* **2006**, *58*, 131–184.
(42) Karlin, K. D.; Zuberbühler, A. D. Formation, Structure, and Reactivity of Copper Dioxygen Complexes In *Bioinorganic Catalysis*, 2nd ed.; Reedijk, J., Bouwman, E., Eds.; Marcel Dekker: New York, 1999; pp 469−534.
(43) Karlin, K. D.; Kaderli, S.; Zuberbühler, A. D. *Acc. Chem. Res.* **1997**, *30*, 139–147.
(44) Yamaguchi, S.; Wada, A.; Funahashi, Y.; Nagatomo, S.; Kitagawa, T.; Jitsukawa, K.; Masuda, H. *Eur. J. Inorg. Chem.* **2003**, *437*, 8–4386.
(45) Wada, A.; Honda, Y.; Yamaguchi, S.; Nagatomo, S.; Kitagawa, T.; Jitsukawa, K.; Masuda, H. *Inorg. Chem.* **2004**, *43*, 5725–5735.

Chart 1

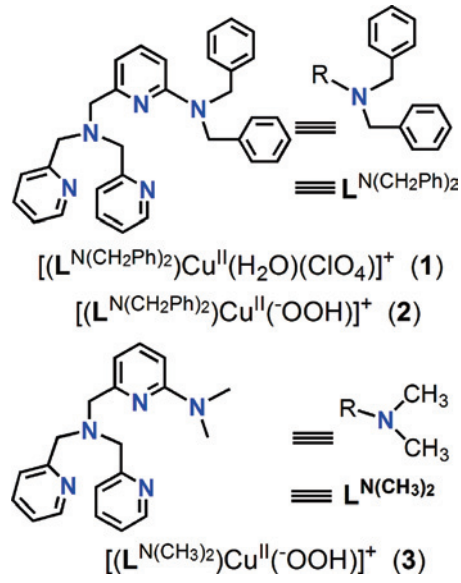

Chart 2

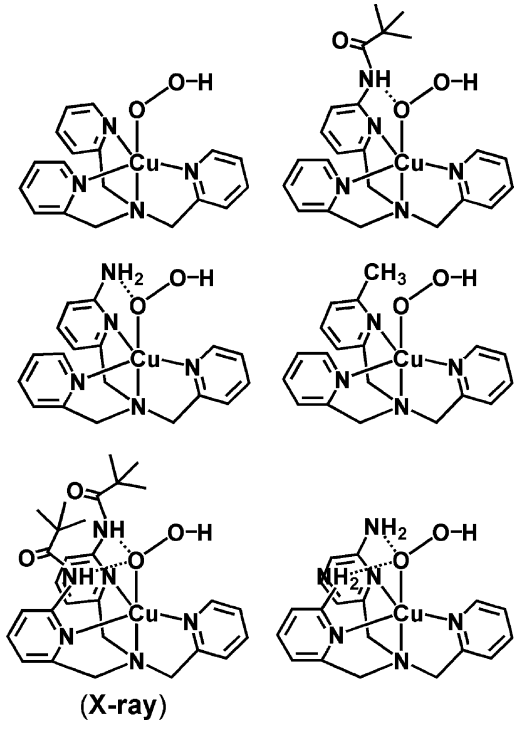

scopic properties due to H bonding.[44,45] Furthermore, Masuda generated a variety of hydroperoxo−copper(II) complexes via (ligand−Cu^{II} + H_2O_2 + base) reactions, including those shown in Chart 2.[33–36] As indicated, one of these could be characterized by X-ray crystallography.[33]

However, the oxidative reactivity of these mononuclear $Cu^{II}(^{-}OOH)$ species (with tetradentate chelates) toward exogenous substrates was not observed. One reason for such inactivity could be that potential substrates could not achieve an appropriate proximity (either spatially or temporarily) to the $Cu^{II}(^{-}OOH)$ moiety. Another explanation could be that the stabilization of the $Cu^{II}(^{-}OOH)$ unit with H bonding comes at the cost of reactivity. Concerning hydroperoxo−Cu(II)

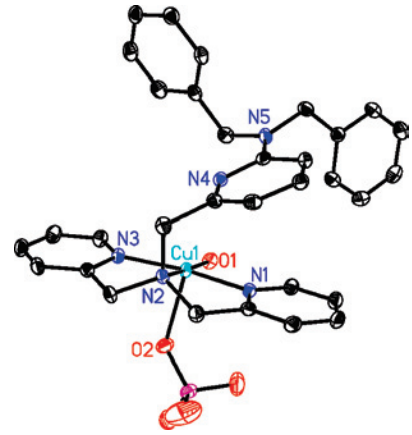

Figure 2. ORTEP diagram of $[(L^{N(CH_2Ph)_2})Cu^{II}(H_2O)(ClO_4)](ClO_4)$ (**1**). Thermal ellipsoids are drawn by ORTEP and represent 50% probability surfaces. Cu(1)−O(1) = 1.9723(11), Cu(1)−N(1) = 1.9885(12), Cu(1)−N(3) = 1.9965(12), Cu(1)−N(1) = 2.0104(12), and Cu(1)−N(4) = 2.935 Å; ∠O(1)−Cu(1)−N(1) = 94.34(5), ∠O(1)−Cu(1)−N(3) = 99.06(5), and ∠N(1)−Cu(1)−N(3) = 166.31(5)°.

compounds, we reported two examples in the last year in which we mounted a potentially oxidizable substrate within the ligand framework, $N(CH_3)_2$, that is, $L^{N(CH_3)_2}$ (Chart 1)[27] or a hydrocarbon aryl group,[26] thus fixed by covalent bonding to be potentially juxtaposed to a $Cu^{II}(^{-}OOH)$ moiety or a species derived from it via O−O cleavage. As mentioned in the Introduction, we detail the overall oxidative copper ion chemistry with $L^{N(CH_2Ph)_2}$.

Copper(II) Complex $[(L^{N(CH_2Ph)_2})Cu^{II}(H_2O)(ClO_4)]ClO_4$ (1). For the purpose of generating a hydroperoxo complex by starting with Cu(II) and adding H_2O_2, we straightforwardly synthesized complex **1**. (See Experimental Section.) X-ray-quality crystals were obtained, and the structure is described here (Figure 2).

The copper(II) ion is five-coordinate. The oxygen atom O(1) from a water molecule along with the alkylamino nitrogen N(2) and pyridyl groups that are not substituted in the 6 position (N(1) and N(3)) comprise the basal plane of the structure found in pyramidal geometry around a copper center. One of the two perchlorate anions coordinates as the fifth axial ligand, $Cu(1)-O(2)_{perchlorate}$ = 2.3515(11) Å. A simple geometric analysis indicates that the overall coordination geometry is a slightly distorted square pyramid (τ = 0.156, where τ = 0.00 for a perfect square pyramid and τ = 1.00 for a trigonal bipyramid).[46] The copper ion (Cu(1)) lies in the best least-squares basal plane. The pyridyl substituents arm (with N(4)) is moved and twisted away from the copper ion (Cu···N(4) = 2.9345(13) Å), most likely because of steric issues with the 6-dibenzylamino substituent.[40,47] The structure is likely maintained in the solution because a typical axial EPR is observed (Figure 3a).

Hydrogen Peroxide Reactivity of $[(L^{N(CH_2Ph)_2})Cu^{II}(H_2O)(ClO_4)]ClO_4$ (1). Generation of $[(L^{N(CH_2Ph)_2})Cu^{II}(^{-}OOH)]^{+}$ (2). The green product solution that forms following the addition of 2 to 3 equiv of H_2O_2/Et_3N using

(46) Addison, A. W.; Rao, T. N.; Reedijk, J.; van Rijn, J.; Verschoor, G. C. *J. Chem. Soc., Dalton Trans.* **1984**, 1349–1356.
(47) Maiti, D.; Woertink, J. S.; Vance, M. A.; Milligan, A. E.; Narducci Sarjeant, A. A.; Solomon, E. I.; Karlin, K. D. *J. Am. Chem. Soc.* **2007**, *129*, 8882–8892.

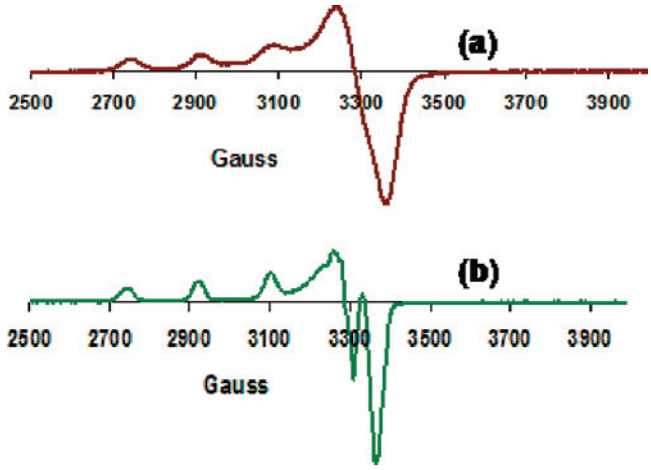

Figure 3. EPR (X band, 77 K, acetone) spectra of (a) $[(L^{N(CH_2Ph)_2})Cu^{II}(H_2O)(ClO_4)](ClO_4)$ (**1**) ($g_{||} = 2.252$, $g_{\perp} = 2.047$, $A_{||} = 170$ G, $A_{\perp} = 29.5$ G) and (b) $[(L^{N(CH_2Ph)_2})Cu^{II}(^{-}OOH)](ClO_4)$ (**2**) generated from the reaction of complex **1** with H_2O_2 ($g_{||} = 2.240$, $g_{\perp} = 2.041$, $A_{||} = 180$ G, $A_{\perp} = 27$ G).

50% H_2O_2(aq) to a greenish-blue acetone solution of complex **1** at −80 °C is formulated as the hydroperoxide species $[(L^{N(CH_2Ph)_2})Cu^{II}(^{-}OOH)]^{+}$ (**2**). The band at $\lambda_{max} = 380$ nm ($\varepsilon = 1400$ $M^{-1}cm^{-1}$) is assignable to a $^{-}OOH-$ > Cu^{II} LMCT absorption on the basis of the correspondence with a number of literature examples.[27,33–37] An axial Cu^{II} EPR spectrum is also observed for complex **2**, which is consistent with a single mononuclear species formulation but is distinguishable from complex **1** (Figure 3b).

Direct evidence of $[(L^{N(CH_2Ph)_2})Cu^{II}(^{-}OOH)]^{+}$ (**2**) comes from ESI-MS. The injection of a −80 °C acetone solution of complex **2** produces a highest-molecular-weight parent-peak cluster with $m/z = 581.03$ and an expected $^{63,65}Cu$ pattern, corresponding to the monocation as formulated. As indicated (Figure 4a), the most prominent ESI-MS peak at $m/z = 548.59$ matches a complex that has lost (H)OOH, $[(L^{N(CH_2Ph)_2})Cu^{II}]^{+}$. When the formation of complex **2** was carried out using $H_2{}^{18}O_2$ instead, the positive ion peak shifted to 585.09 because of the formation of $[(L^{N(CH_2Ph)_2})Cu^{II}(^{-}{}^{18}O{}^{18}OH)]^{+}$ (**2-^{18}O**); the fitting of the parent peak pattern around $m/z = 585$ indicates >99% ^{18}O incorporation.

Hydrogen peroxide or ^{-}OOH is known to attack the carbonyl group of acetone, and Itoh and coworkers[21] recently observed a thus-formed alkylperoxo adduct bound to copper(II) in related but tridentate ligand−copper complex chemistry. However, by ESI-MS, we see no evidence of such a hydroperoxo−acetone−copper(II) complex. Also, see the further discussion below.

Ligand Oxidative Reactivity for $[(L^{N(CH_2Ph)_2})Cu^{II}(^{-}OOH)]^{+}$ (2). Hydroperoxo−copper(II) species **2** is stable in solution at −80 °C, but a warming results in a change to a darker-green color. Thin-layer chromatography and ESI-MS data obtained from the product solution that has been stripped of copper ion (by the addition of Na_2EDTA(aq) and an extraction into CH_2Cl_2; see Experimental Section) shows that the formation of several new organic products has occurred. Thus, the singly N-dealkylated (i.e., N-debenzylation) compound $L^{NH(CH_2Ph)}$ ($m/z = 396.48$ (M + H), 418.49 (M + Na)), the singly oxygenated organic compound $L^{N(CH_2Ph)(COPh)}$ ($m/z = 500.32$ (M + H), 522.35 (M + Na)), the overoxidized/oxygenated amide derived from benzoic acid $L^{NH(COPh)}$ ($m/z = 410.47$ (M + H), 432.41 (M + Na)), and the doubly oxygenated (bis-amide) parent ligand $L^{N(COPh)_2}$ ($m/z = 514.22$ (M + H), 536.27 (M+Na)) are present. Unreacted ligand $L^{N(CH_2Ph)_2}$ ($m/z = 486.36$ (M + H), 418.49 (M + Na)) is also present. The absolute yields (average of three runs) are summarized in Scheme 2.

We also observed overoxidized products, that is, more than the single two-electron substrate oxidation (peroxide as an oxidizing/oxygenating agent) in our previously published results with $L^{N(CH_3)_2}$ and $[(L^{N(CH_3)_2})Cu^{II}(^{-}OOH)]^{+}$ (**3**).[27] However, here no corresponding L^{NH_2} product derived from complex **2** was observed. In the present chemistry, chromatographic separation/isolation reveals that only ∼16% yield of the original $L^{N(CH_2Ph)_2}$ ligand remains after reactions. The major (∼48%) new organic product formed is the oxidatively singly N-debenzylated compound $L^{NH(CH_2Ph)}$ (Scheme 2). As would be expected in an N-dealkylation reaction, a corresponding aldehyde should form, and indeed we observe ∼43% yield of benzaldehyde as determined by GC and GC-MS spectroscopy. When labeled hydrogen peroxide is used in the reaction that gives $[(L^{N(CH_2Ph)_2})Cu^{II}(^{-}{}^{18}O{}^{18}OH)]^{+}$ (**2-^{18}O**), ^{18}O-labeled PhC(^{18}O)H is formed, and ∼65% of the theoretically expected ^{18}O is incorporated. Benzaldehyde, with its fairly exchangeable (with water) carbonyl group, is well documented in not always retaining a high degree of ^{18}O incorporation.[48,49] As mentioned and from the yields obtained (Scheme 2), small but significant amounts of formally four- or eight-electron overoxidized products form, including ketones $L^{N(CH_2Ph)(COPh)}$ plus $L^{N(COPh)_2}$ (7%) and $L^{NH(COPh)}$ (3%) (Scheme 2). These are likely derived from the reaction of the initial two-electron oxidation products with an excess of hydrogen peroxide. (Also, see below.)

When only 1 equiv of H_2O_2/Et_3N is used to generate $[(L^{N(CH_2Ph)_2})Cu^{II}(^{-}OOH)]^{+}$ (**2**), a warming and a workup lead to considerably more (∼65%) unreacted $L^{N(CH_2Ph)_2}$, and the yield of primary mono-N-debenzylated ligand−substrate $L^{NH(CH_2Ph)}$ drops to 16%; only 1% (total) of $L^{N(CH_2Ph)(COPh)}$ plus $L^{N(COPh)_2}$ is obtained. No $L^{NH(COPh)}$ or L^{NH_2} is observed. Thus, the major reaction product is again the two-electron (from one H_2O_2) oxidatively N-dealkylated $L^{NH(CH_2Ph)}$, which is formed in a dose-dependent manner. Furthermore, following our comments above, we wanted to rule out the possible involvement of a solvent in activating the hydroperoxo species. Thus, we carried out the formation of $[(L^{N(CH_2Ph)_2})Cu^{II}(^{-}OOH)]^{+}$ (**2**) in both propionitrile and methanol solvents, separately. In both cases, product distributions were found to be similar to those found for acetone. We conclude that the $Cu^{II}(^{-}OOH)^{+}$ moiety truly affects the oxidations observed.

Some further insights into the overall chemistry occurring in this system come from the direct ESI-MS reaction solution following the warming to room temperature but prior to the extraction of the copper ion with EDTA (vide supra). The ESI-MS data (in Supporting Information) reveal the presence of several copper complexes, $[(L^{NH(CH_2Ph)})Cu]^{+}$ ($m/z = 457.48$) and

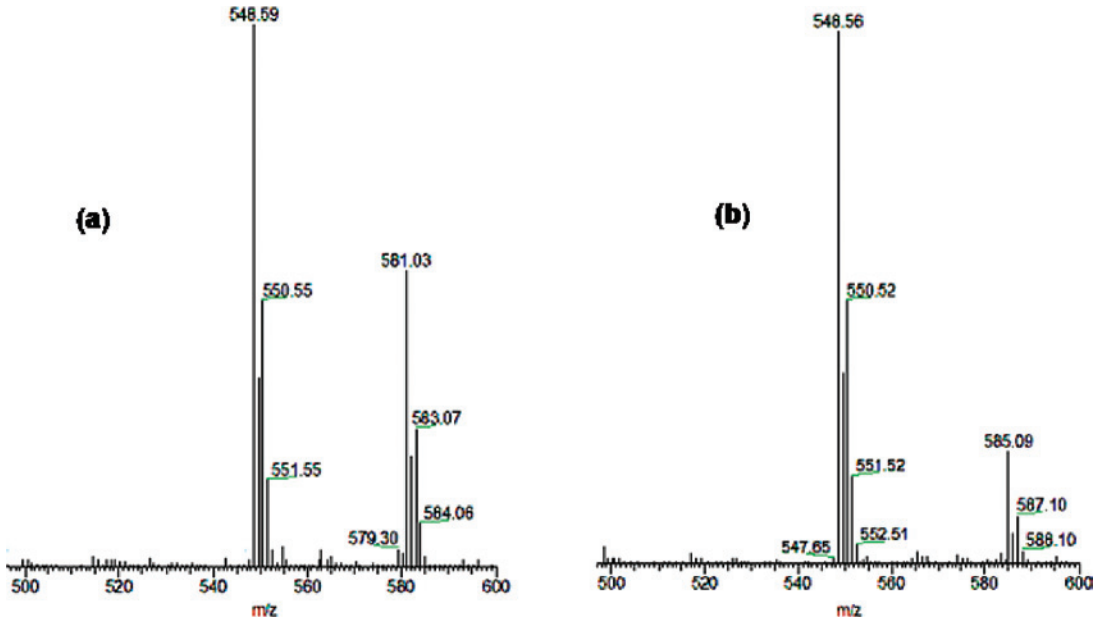

Figure 4. ESI-MS spectra of (a) $[(L^{N(CH_2Ph)_2})Cu^{II}(^{-}OOH)](ClO_4)$ (**2**) from the reaction of complex **1** with H_2O_2 and (b) $[(L^{N(CH_2Ph)_2})Cu^{II}(^{-18}O^{18}OH)](ClO_4)$ (**2-^{18}O**) generated by complex **1**/$H_2{}^{18}O_2$.

Scheme 2

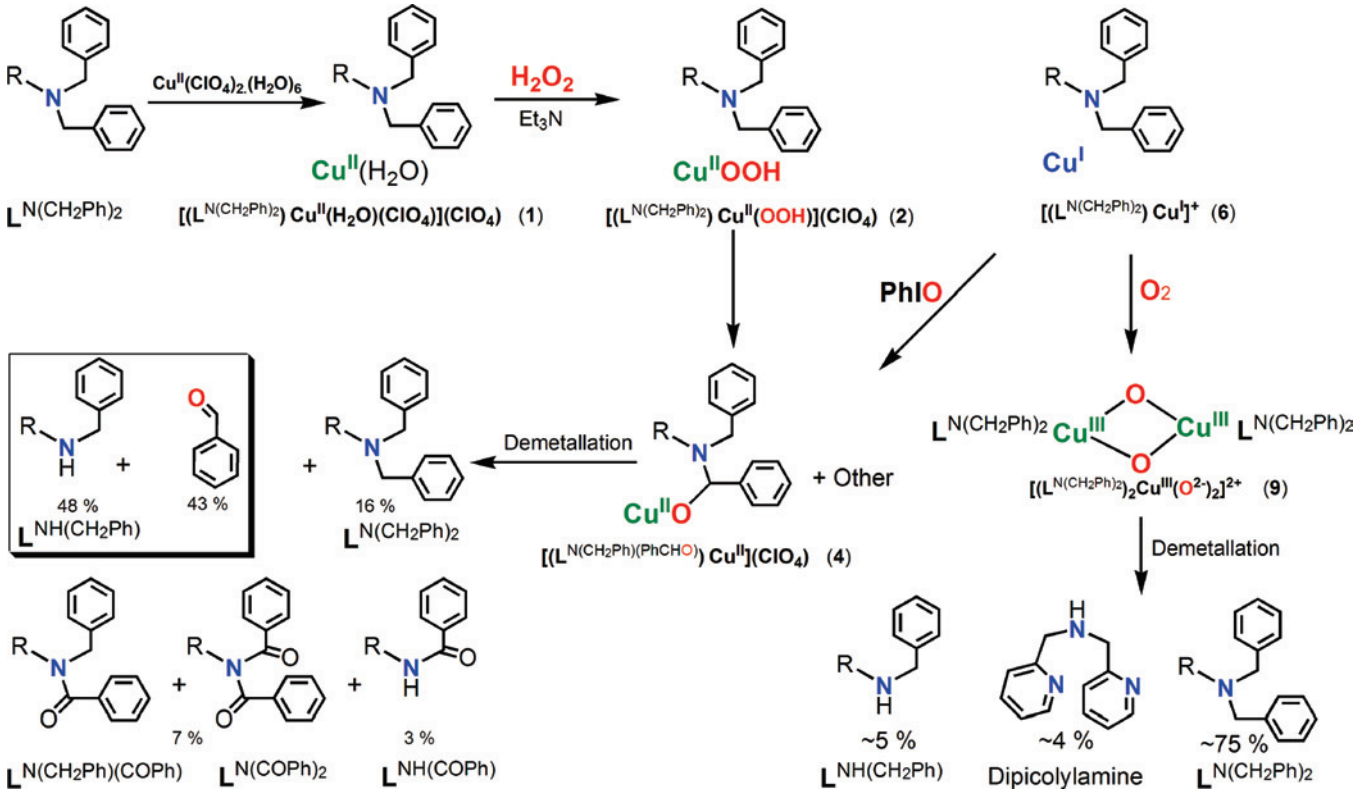

$[(L^{NH(CH_2Ph)})Cu(acetone)]^+$ (m/z = 517.27) (unreacted $[(L^{N(CH_2Ph)_2})Cu]^+$ (m/z = 548.53)). In addition, a prominent (intense) ESI-MS cluster is found at m/z = 563.05, which corresponds to alkoxide species $[(L^{N(CH_2Ph)(PhCHO^-)})Cu^{II}]^+$ (**4**); see Scheme 2. In a corresponding experiment with $[(L^{N(CH_2Ph)_2})Cu^{II}(^{-18}O^{18}OH)]^+$ (**2-^{18}O**), ^{18}O does appear in this alkoxide product, $[(L^{N(CH_2Ph)(PhCH(18)O^-)})Cu]^+$ (m/z = 565.19; 94% ^{18}O incorporation). As will be described below, this finding is relevant to the biomimetic nature of the reaction chemistry and also provides some insight into mechanistic considerations.

X-ray Crystal Structure of $[(L^{NH(CH_2Ph)})Cu^{II}(Cl)]ClO_4$ (10). We wish to verify further our major organic product assignment, and thus for $L^{NH(CH_2Ph)}$ that was isolated and purified via column chromatography, we formed a copper-complex product. Under Ar, the reaction of $L^{NH(CH_2Ph)}$ and $Cu^I(MeCN)_4(ClO_4)$ in acetonitrile followed by the addition of $CHCl_3$ leads to the chloro−copper(II) complex

(48) Lee, D.; Lippard, S. J. *Inorg. Chem.* **2002**, *41*, 827–837.

$[(L^{NH(CH_2Ph)})Cu^{II}(Cl)]^+$ (**10**). (See Experimental Section.) An X-ray structure of the pentacoordinate complex was obtained (see the diagram), and it confirms the presence and the identity of $L^{NH(CH_2Ph)}$. The full X-ray structure is presented in the Supporting Information.

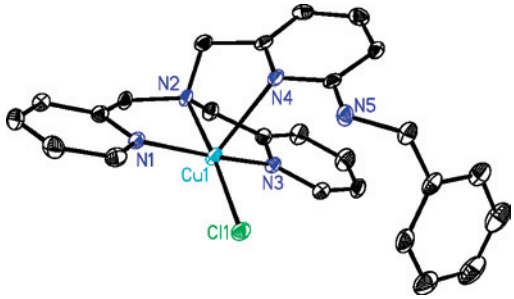

Corresponding Cu^I/O_2 Chemistry with $L^{N(CH_2Ph)_2}$. Whereas the results that were presented so far implicate the $Cu^{II}(^-OOH)$ moiety as being responsible for the observed reactivity (Scheme 2), as before,[27] we have examined the products of the O_2 reaction with $[(L^{N(CH_2Ph)_2})Cu^I]B(C_6F_5)_4$ (**6**) to determine if copper(I)−dioxygen might be responsible. This does not seem to be the case (vide infra).

In the context of other work, the complex **6**/O_2 reactions result in the formation of the metastable bis(μ-oxo)dicopper(III) complex, $[((L^{N(CH_2Ph)_2})Cu^{III})_2(O^{2-})_2](B(C_6F_5)_4)_2$ (**9**), which could be characterized by low-temperature UV−vis and rR spectroscopy.[39] By warming such solutions to room temperature and following $Na_2EDTA/H_2O/CH_2Cl_2$ demetalation procedures, we found the organic products and yields of these (which are low) to be quite different from the $[(L^{N(CH_2Ph)_2})Cu^{II}(H_2O)(ClO_4)]^+$ (**1**)/H_2O_2/Et_3N chemistry (Scheme 2). Some of the oxidative N-dealkylation product $L^{NH(CH_2Ph)}$ is observed but in only ∼5% total yield. A small amount of new product dipicolylamine (∼4% yield) is also observed; this must be derived from the $Cu^{III}_2(O^{2-})_2$ attack on the benzylic position of the substituted (i.e., with $N(CH_2Ph)_2$) pyridyl moiety, which is analogous to that previously seen by Suzuki and coworkers.[50,51] Most of the recovered organic (∼75%) is unreacted starting ligand $L^{N(CH_2Ph)_2}$ (Scheme 2). The Cu^I/O_2 reaction would normally progress through a copper−superoxo $[Cu^{II}(O_2^-)]$ initial species,[6,7] thus the observed oxidative chemistry of $[(L^{N(CH_2Ph)_2})Cu^{II}(H_2O)(ClO_4)]^+$ (**1**)/H_2O_2/Et_3N does not proceed via a superoxo species. The lack of an effective N-debenzylation reaction of $L^{N(CH_2Ph)_2}$ by $[Cu^{III}_2(O^{2-})_2]^{2+}$ is most likely due to the axial positioning of the *N*,*N*-dibenzyl arm that prevents the oxo-atom attack. Suzuki and coworkers demonstrated such an axial ligand elongation for 6-substituted 2-pyridyl ligand arms in $[((6\text{-}Me_2TPA)Cu^{III})_2(O^{2-})_2]^{2+}$ (X-ray, Me_2TPA is (2-pyridylmethyl)bis(6-methyl-2-pyridylmethyl)amine).[50]

Reaction of $[(L)Cu^I]^+$ with PhIO. One might anticipate that $[(L^{N(CH_2Ph)_2})Cu^{II}(^-OOH)]^+$ (**2**) could potentially undergo O−O cleavage chemistry and give a high-valent copper−oxo species, something that is sought after but unknown. (See further discussion below.) There is a very broad and more established Fe^{III}−OOR (R = H, alkyl, or acyl; either heme or nonheme iron) homolytic or heterolytic O−O cleavage (bio)chemistry.[52–57] In this context, iodosylbenzene or analog donors have been widely utilized with reduced metal complexes to generate higher-valent metal−oxo complexes (i.e., PhIO + ligand−M^{n+}; (M = heme or nonheme Fe, Mn, etc.) → ligand−M^{n+2} = (O^{2-}) + PhI).[58–61] As referred to in the Introduction, a copper−oxo moiety is seen either to be responsible for the H atom abstraction in PHM or DβM or to form later in the reaction sequence/mechanism.

In fact, we were previously successful in affecting the C−H activation and the ligand methyl group hydroxylation, leading to an alkoxo product $[(TMG_3trenO^-)Cu^{II}]^+$; see the diagram ($TMG_3tren$ is tris(2-(*N*-tetramethylguanidyl)ethyl)amine).[24]

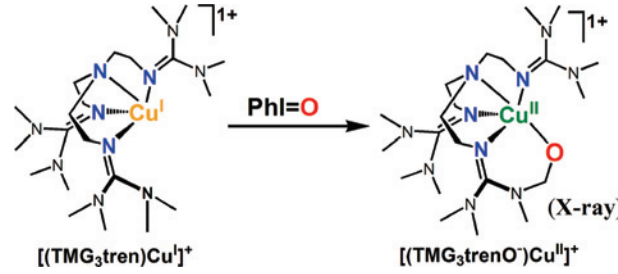

Most interestingly, for the present system, the reaction of PhIO with the cuprous complex $[(L^{N(CH_2Ph)_2})Cu^I]^+$ (**6**) did produce $[(L^{N(CH_2Ph)(PhCHO^-)})Cu^{II}]^+$ (**4**) (Scheme 2), as detected by ESI-MS (m/z = 563.18) and as corroborated when employing $PhI^{18}O$ (m/z = 565.34) because of $[(L^{N(CH_2Ph)(PhCH(18)O^-)})Cu^{II}]^+$ (**4-^{18}O**) in complementary experiments. (See Supporting Information.) One thus could suggest that the cupryl species $[(L^{N(CH_2Ph)_2})Cu^{II}{-}O\bullet]^+$ (**8**) formed during the reaction and affected the hydroxylation. However, caution is required because it is possible that an iodosylbenzene-bound copper complex (e.g., $[(L^{N(CH_2Ph)_2})Cu^I{-}OIPh]^+$) is the true oxygenating agent and that prior O−O cleavage did not occur.

Potentially exciting observations occurred when we followed the $[(L^{N(CH_2Ph)_2})Cu^I]^+$ (**6**)/PhIO chemistry using ESI-MS as a function of time; the reaction was carried out at −40 °C, and aliquot samples were injected into the mass spectrometer while initially at this temperature. Most interestingly, early on in the reaction, ∼1 min after the addition of PhIO to $[(L^{N(CH_2Ph)_2})Cu^I]^+$ (**6**) (CH_3CN solvent, −40 °C), the predominant detected higher-molecular-weight ESI-MS species occurs with the strongest peak at m/z = 564.25

(49) Greenzaid, P.; Luz, Z.; Samuel, D. *Trans. Faraday Soc.* **1968**, *64*, 2780–2786.
(50) Hayashi, H.; Fujinami, S.; Nagatomo, S.; Ogo, S.; Suzuki, M.; Uehara, A.; Watanabe, Y.; Kitagawa, T. *J. Am. Chem. Soc.* **2000**, *122*, 2124–2125.
(51) Mizuno, M.; Honda, K.; Cho, J.; Furutachi, H.; Tosha, T.; Matsumoto, T.; Fujinami, S.; Kitagawa, T.; Suzuki, M. *Angew. Chem., Int. Ed.* **2006**, *45*, 6911–6914.
(52) Shan, X.; Que, L., Jr *J. Inorg. Biochem.* **2006**, *100*, 421–433.
(53) Costas, M.; Mehn, M. P.; Jensen, M. P.; Que, L., Jr *Chem. Rev.* **2004**, *104*, 939–986.
(54) Soper, J. D.; Kryatov, S. V.; Rybak-Akimova, E. V.; Nocera, D. G. *J. Am. Chem. Soc.* **2007**, *129*, 5069–5075.
(55) Nam, W.; Han, H. J.; Oh, S. Y.; Lee, Y. J.; Choi, M. H.; Han, S. Y.; Kim, C.; Woo, S. K.; Shin, W. *J. Am. Chem. Soc.* **2000**, *122*, 8677–8684.

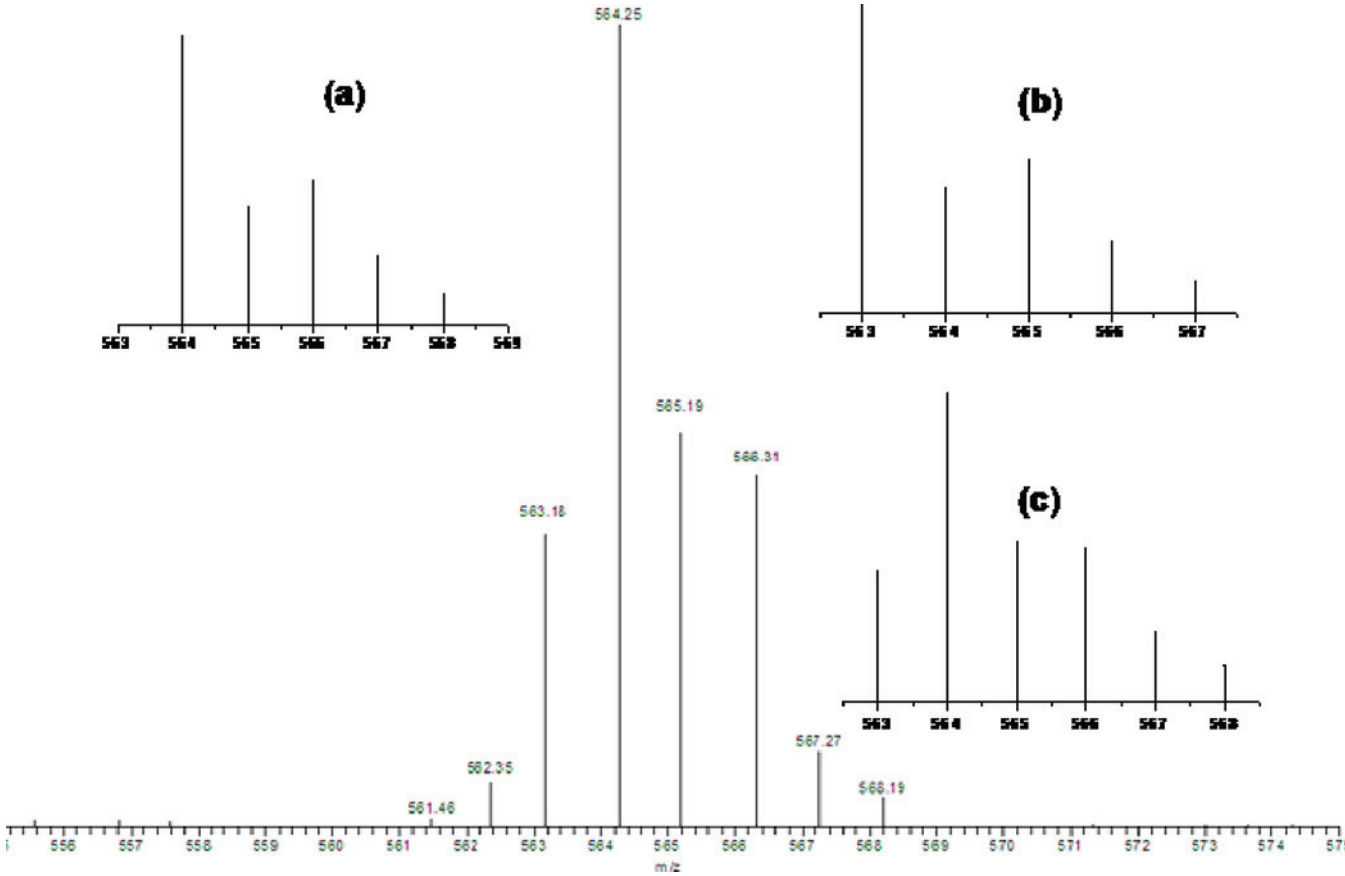

Figure 5. ESI-MS spectra from the reaction of $[(L^{N(CH_2Ph)_2})Cu^{I}]^{+}$ (**6**) with PhIO, suggesting the transient formation of the cupryl complexes $[(L^{N(CH_2Ph)_2})Cu^{II}{-}O\bullet]^{+}$ (**8**) at m/z = 564.25 (~70% formation) and $[(L^{N(CH_2Ph)(PhCHO^{-})})Cu^{II}]^{+}$ (**4**) at m/z = 563.18 (~30% formation). Insets showing the expected pattern for (a) 100% formation of complex **8** and (b) 100% formation of complex **4** and (c) the best fit to the data with 70% formation of complex **8** plus 30% formation of complex **4**. See the text for further discussion.

(Figure 5), which in fact corresponds to a cupryl species, $[(L^{N(CH_2Ph)_2})Cu^{III}{=}O]^{+}$ (complex **8**, $Cu^{III}{=}O \equiv Cu^{II}{-}O\bullet$). This peak is observed only early on as the product alkoxo complex $[(L^{N(CH_2Ph)(PhCHO^{-})})Cu^{II}]^{+}$ (**4**) (m/z = 563.18) comes in and dominates. Notice that the theoretical fitting of this early-time mass spectrum best corresponds to a mixture of 70% cupryl (complex **8**) and 30% alkoxo product **4** (Figure 5). In the Supporting Information, we show a succession of mass spectra (as a function of time) that demonstrates how the putative cupryl is there initially but disappears after ~5 to 6 min; it is almost absent after ~3 min. The yields of the organics from the reaction of $[(L^{N(CH_2Ph)_2})Cu(I)]B(C_6F_5)_4$ (**6**) with PhIO could not be determined because of insufficient separation and tailing observed in column and thin-layer chromatography.

Similarly, we carried out a PhIO reaction with the previously studied ligand complex with dimethylamino substituents/substrate, $[(L^{N(CH_3)_2})Cu^{I}]^{+}$ (**7**).[27,39] Electrospray ionization mass spectrometry data indicate that the corresponding alokoxide product forms (i.e., $[(L^{N(CH_3)(CH_2O^{-})})Cu^{II}]^{+}$ (**5**) (m/z = 411.18)). (See Supporting Information.) This also forms from $[(L^{N(CH_3)_2})Cu^{II}(^{-}OOH)]^{+}$ (**3**) chemistry, as reported.[27] Interestingly, when the partially deuteriated ligand complex $[(L^{N(CH_3)(CD_3)})Cu^{I}]^{+}$ (**7-CD$_3$**) was reacted with PhIO, the ESI-MS analysis lead to the conclusion that for this reaction the kinetic isotope effect (k_H/k_D) is 1.9 on the basis of the relative formation of $[(L^{N(CD_3)(CH_2O^{-})})Cu^{II}]^{+}$ (m/z = 414.14) and $[(L^{N(CH_3)(CD_2O^{-})})Cu^{II}]^{+}$ (m/z = 413.24) (Figure 6). This may be compared to the finding that $k_H/k_D \approx 2.2$ for the $[(L^{N(CH_3)(CD_3)})Cu^{II}(^{-}OOH)]^{+}$ (**3**) reaction.[27] Considering that 1.9 and 2.2 are nearly within the experimental error we suggest that both the $[(L)Cu^{II}(^{-}OOH)]^{+}$ and $[Cu^{I}]^{+}$/PhIO chemistries proceed through a common reactive intermediate, the cupryl species $[(L)Cu^{II}{-}O\bullet]^{+}$. (See the diagram.) The data are suggestive but are probably not yet good enough to firmly establish cupryl chemistry.

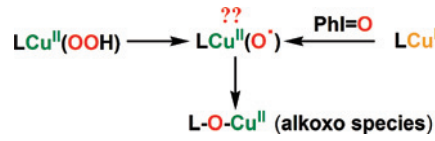

To summarize this section of the discussion, we employed PhIO reactions with reduced complexes $[(L)Cu^{I}]^{+}$ to probe the possibility that high-valent cupryl species are involved in the reactions of $[(L)Cu^{II}(^{-}OOH)]^{+}$ (i.e., following hemolytic O−O bond cleavage). For both the ligand complexes with $L^{N(CH_2Ph)_2}$ and $L^{N(CH_3)_2}$, PhIO reactions do produce the expected alkoxo products (Scheme 2), and the mass spectrometric data (Figure 5) appear to give direct evidence of the presence or the formation of the cupryl complex for one case, $[(L^{N(CH_2Ph)_2})Cu^{II}O\bullet]^{+}$ (**8**). We do not wish to state overly strongly that we have detected the first copper cupryl. The overall reaction yields are not exceptional for the PhIO

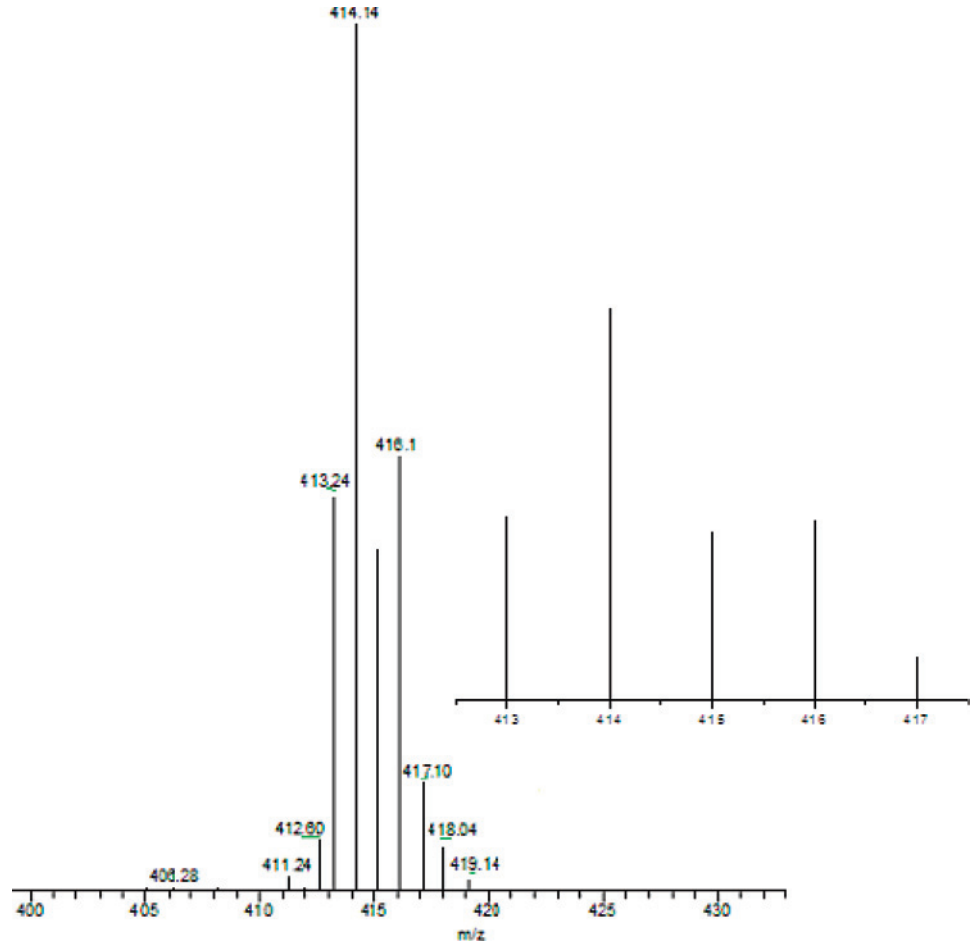

Figure 6. ESI-MS spectra obtained from the reaction of $[(L^{N(CH_3)(CD_3)})Cu^{I}]^{+}$ (**7**) with PhIO. The ratio of formation of $[(L^{N(CD_3)(CH_2O^{-})})Cu^{II}]^{+}$ (m/z = 414.14) versus that of $[(L^{N(CH_3)(CD_2O^{-})})Cu^{II}]^{+}$ (m/z = 413.24) suggests that $k_H/k_D \approx 1.9$. The inset shows the expected (calculated) ESI-MS spectral pattern for a reaction that would lead to $k_H/k_D \approx 1.9$.

Scheme 3

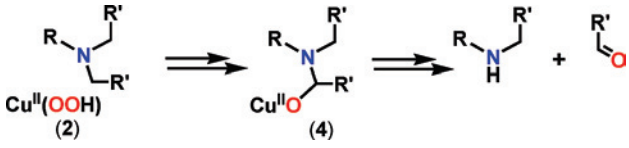

Scheme 4

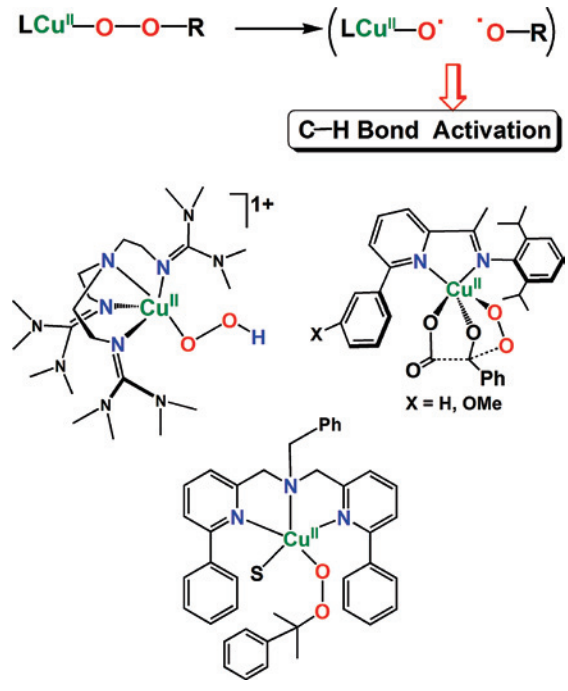

reaction chemistry, although this is probably not the ideal oxo transfer agent. Also, whereas we detected the cupryl species in the ESI-MS experiments by using PhIO, for some reason, it was not observed when employing $PhI^{18}O$; however, that final product alkoxide did contain ^{18}O. In addition to the chemistry described here (and the initial Article),[27] $Cu^{II}-O-OR$ homolytic cleavage has been suggested to lead to a $Cu^{II}-O\bullet$ transient reactive species that may affect substrate oxidation/oxygenation chemistry.[20,22,24,62–64] Scheme 4 depicts some of the recent synthetic examples.[20,22,27]

Mechanistic Discussion. Oxidative N-dealkylation is a relatively common reaction in the biotransformation of alkylamines; it is also catalyzed by cytochrome P450 monooxygenases. Considerable experimental effort has gone into differentiating between conventional hydrogen atom transfer (HAT) and a sequential reaction in which single-electron-transfer (SET) oxidation is followed by deprotonation.[57,65–67] Oxidative N-dealkylation of the ligand bound to copper in $Cu^{III}_2(O^{2-})_2$ compounds has been observed where mechanistic studies favored initial HAT.[7]We also

Scheme 5

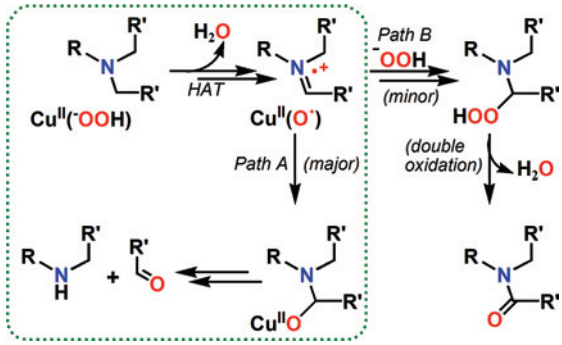

have reported on cases where a $Cu^{III}_2(O^{2-})_2$ (or side-on-bound peroxo−dicopper(II) species in equilibrium with this) oxidatively N-dealkylates substituted dimethylanilines but where a shift in mechanism from ET to HAT was observed, depending on the ease of substrate one-electron oxidation.[68]

As discussed above for the complexes' N,N-dimethyl groups at the 6-position of one arm of the TMPA-derived ligand, observed KIE values are ∼2.2 for $[(L^{N(CH_3)(CD_3)})Cu^{II}(^{-}OOH)]^+$ (**3-CD$_3$**)[27] chemistry and ∼1.9 for $[(L^{N(CH_3)(CD_3)})Cu^{I}]^+$ (**7-CD$_3$**)/PhIO chemistry. These results suggest that a net H atom abstraction occurs. Organic products isolated (i.e., recovered dialkyl ligand) from $[(L^{N(CH_3)(CD_3)})Cu^{II}(^{-}OOH)]^+$ chemistry included those due to the scrambling of isotopes via radical intermediates, and $L^{N(CH_3)(CD_3)}$, $L^{N(CH_3)(CD_2H)}$, $L^{N(CH_3)(CDH_2)}$, and $L^{N(CH_3)_2}$ were all observed. However, more studies would be required to differentiate between HAT and a SET step.

On the basis of the results described here, we outline our proposed mechanism of the reaction for $[(L^{N(CH_2R')_2})Cu^{II}(^{-}OOH)]^+$ chemistry (Scheme 5). The initial net HAT (occuring either directly from the hydroperoxide or following O−O cleavage) substrate H atom abstraction would lead to a high-valent $Cu^{II}-O^{\bullet}$ (also $Cu^{III}=O$) and substrate iminium radical cation species; rebound produces the alkoxide (Path A). Most often in the synthetic system and always in the enzyme, protonation (from active-site solvent) releases the organic products observed, the amine and the corresponding aldehyde.

(56) Traylor, T. G.; Traylor, P. S. Reactions of Dioxygen and Its Reduced Forms with Heme Proteins and Model Porphyrin Complexes In *Active Oxygen in Biochemistry*; Valentine, J. S., Foote, C. S. , Greenberg, A., and Liebman, J. F., Eds.; Chapman & Hall: New York, 1995; pp 84−187.

(57) Meunier, B.; de Visser, S. P.; Shaik, S. *Chem. Rev.* **2004**, *104*, 3947–3980.

(58) Que, L., Jr *Acc. Chem. Res.* **2007**, *40*, 493–500.

(59) McLain, J. L.; Lee, J.; Groves, J. T. Biomimetic Oxygenations Related to Cytochrome P450: Metal-Oxo and Metal-Peroxo Intermediates In *Biomimetic Oxidations Catalyzed by Transition Metal Complexes*; Meunier, B., Ed.; Imperial College Press: London, 2000; pp 91−169.

(60) Song, W. J.; Seo, M. S.; DeBeer George, S.; Ohta, T.; Song, R.; Kang, M.-J.; Tosha, T.; Kitagawa, T.; Solomon, E. I.; Nam, W. *J. Am. Chem. Soc.* **2007**, *129*, 1268–1277.

(61) Qin, K.; Incarvito, C. D.; Rheingold, A. L.; Theopold, K. H. *J. Am. Chem. Soc.* **2002**, *124*, 14008–14009.

(62) Chen, P.; Fujisawa, K.; Solomon, E. I. *J. Am. Chem. Soc.* **2000**, *122*, 10177–10193.

(63) Comba, P.; Knoppe, S.; Martin, B.; Rajaraman, G.; Rolli, C.; Shapiro, B.; Stork, T. *Chem.−Eur. J.* **2008**, *14*, 344–357.

(64) Klinman, J. P. *Chem. Rev.* **1996**, *96*, 2541–2561.

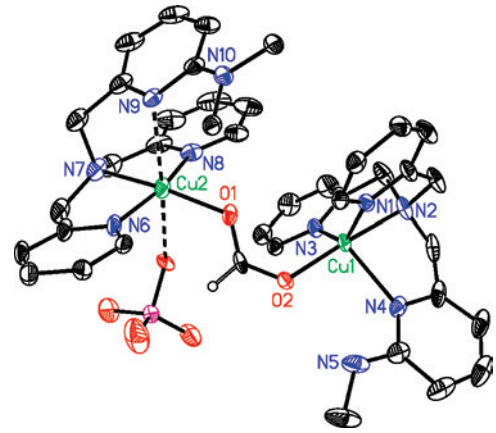

Figure 7. ORTEP diagram of the cationic component of $[(L^{N(CH_3)_2})Cu^{II}(HCOO^{-})(ClO_4)Cu^{II}(L^{NH(CH_3)})](ClO_4)_2$ (**11**). Thermal ellipsoids are drawn by ORTEP and represent 50% probability surfaces. Cu(1)−O(2) = 1.42(2), Cu(1)−N(3) = 2.020(3), Cu(1)−N(2) = 2.022(3), and Cu(1)−N(1) = 2.023(3) Å; ∠O(2)−Cu(1)−N(3) = 96.00(11), ∠O(2)−Cu(1)−N(2) = 175.51(13), ∠N(3)−Cu(1)−N(2) = 82.15(12), and ∠O(2)−Cu(1)−N(1) = 99.39(11)°.

In Scheme 5, we also show (Path B) how an overoxidized product amide would most likely form in the model synthetic system via a facile nucleophilic attack of a second equivalent of the hydroperoxide anion. In connection with other overoxidation product chemistry, we recently isolated a small amount of a decomposition product, $[(L^{N(CH_3)_2})Cu^{II}(HCOO^{-})(ClO_4)Cu^{II}-(L^{NH(CH_3)})](ClO_4)_2$ (**11**), for which we were able to obtain an X-ray structure (Figure 7). (See Supporting Information.) This originates from the previously described chemistry of $[(L^{N(CH_3)_2})Cu^{II}(^{-}OOH)]^+$ (**3**). This odd dicopper(II) complex possesses a bridging formate ($HCOO^{-}$) group wherein one of the copper ligands is $L^{N(CH_3)_2}$ (i.e., the unreacted starting ligand), and the other copper ion is supported by the singly N-demethylated product $L^{NH(CH_3)}$. An EPR spectrum of the isolated crystals that were dissolved in acetone indicates the presence of two independent Cu(II) ions with overlapping axial spectra. (See Supporting Information.) Furthermore, an ESI-MS of the material contains two strong peaks: the one at m/z = 427.04 corresponds to $[(L^{NH(CH_3)})Cu^{II}(HCOO^{-})]^+$, and the other at m/z = 441.04 corresponds to $[(L^{N(CH_3)_2})Cu^{II}(HCOO^{-})]^+$. The generation of formate ($HCOO^{-}$) can be envisaged because formaldehyde was previously detected as a product derived from complex **3**. Similarly, we are able to detect a small ESI-MS peak at m/z = 579.17 from the decomposition product mixture of $[(L^{N(CH_2Ph)_2})Cu^{II}(^{-}OOH)]^+$ (**2**), which corresponds to a copper−complex species containing benzoate, $[(L^{NH(CH_2Ph)})Cu^{II}(PhCOO^{-})]^+$ (i.e. a further oxidation product of benzaldehyde, which was a primary product derived from complex **2**). All of these overoxidized products are obtained in very low yields. Nevertheless, they are indicative of the extensive chemistry occurring in the manner proposed.

PAM Chemistry Mimic. We have shown here that the hydroperoxo group reaction in $[(L^{N(CH_2Ph)_2})Cu^{II}(^{-}OOH)]^+$ (**2**) leads to the formation of oxidatively N-dealkylated $L^{NH(CH_2Ph)}$ plus PhCH=O. The $-N(CH_2Ph)_2$ substrate (ligand substituent) resides in close proximity to the $Cu^{II}(^{-}OOH)$ moiety (Scheme 3, R′ = Ph), and essentially

identical chemistry occurs for R′ = H.[27] As described above, a copper(II)−alkoxide complex forms prior to organic product release (Scheme 3).

Thus, the present model systems (R′ = H, Ph) very closely resemble much of the proposed oxidative N-dealkylation reaction mechanism affected by PAM (Figure 1). There, an active-site reactive species forms at Cu_M with His_2Met coordination, which is ideally juxtaposed to the prohormone peptide substrate C−H group of the terminal glycine. Furthermore, our cupric−alkoxide complex, which is formed from $[(L^{N(CH_2Ph)_2})Cu^{II}(^{-}OOH)]^+$ (**2**) or $[(L^{N(CH_2Ph)_2})Cu^{I}]^+$ (**6**)/PhIO reactivity mimics the product substrate Cu^{II}−alkoxide complex discussed for both PHM and DβM. (See the diagram.[9]) However, as stated in the Introduction, the current thought is that a copper−superoxo complex may be the active species or it could be a cupryl species derived from $Cu^{II}(^{-}OOH)$ O−O bond cleavage. Our results, with a reactivity pattern so close to that of PHM/PAM, rather favor the view that the reactive species is a hydroperoxo or cupryl group.

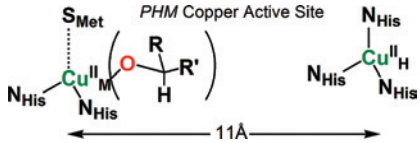

Summary

This Article summarizes our advances in oxidative N-dealkylation chemistry with hydroperoxo−copper(II) complexes that have a dialkylamino substrate ($-N(CH_2Ph)_2$ or $-N(CH_3)_2$) appended as a substituent on one pyridyl group of the tripodal-tetradentate TMPA-ligand framework. In the previous Communication and from the present full Article, we can argue that $Cu^{II}(^{-}OOH)$ or a species generated from it (i.e., a high-valent copper−oxo species) can initiate useful substrate hydroxylation reactions that are occurring in the enzyme PAM (PHM + PAL) (Figure 1). Net substrate H-atom abstraction occurs starting with the $Cu^{II}(^{-}OOH)$ moiety, and the likely structure of an intermediate substrate organic radical species is proposed, which accounts for the observed products. The formation of a substrate and an ^{-}OOH-derived alkoxo $Cu^{II}(^{-}OR)$ complex has been proven; the latter has also been proposed in PHM mechanisms. The fact that the alkoxo complex forms from either $Cu^{II}(^{-}OOH)$ or Cu^{I}/PhIO chemistry suggests the possibility that a high-valent copper−oxo reactive intermediate forms and ESI-MS data provide some further support. Clearly, however, further studies on this or other systems need to be carried out to substantiate truly the existence of a cupryl species and to elucidate the full chemistry of the already-existing $Cu^{II}(^{-}OOH)$ and $Cu^{II}(O_2^{-}\bullet)$ complexes.

Acknowledgment. This work was supported by grants from the National Institutes of Health (K.D.K., GM28962).

Supporting Information Available: X-ray structures with selected bond lengths and angles; ESI−MS and other spectroscopic details. This material is available free of charge via the Internet at http://pubs.acs.org.

IC800617M

(65) *Cytochrome P450: Structure, Mechanism, and Biochemistry,* 3rd ed.; Ortiz de Montellano, P. R., Ed.; Kluwer Academic/Plenum: New York, 2005.

(66) Bhakta, M.; Hollenberg, P. F.; Wimalasena, K. *Chem. Commun.* **2005**, 265–267.

(67) Nehru, K.; Seo, M. S.; Kim, J.; Nam, W. *Inorg. Chem.* **2007**, *46*, 293–298.

(68) Shearer, J.; Zhang, C. X.; Zakharov, L. N.; Rheingold, A. L.; Karlin, K. D. *J. Am. Chem. Soc.* **2005**, *127*, 5469–5483.